Inorg. Chem. **2003**, *42*, 8494–8503

Increased Reactivity of the $^{\bullet}Cr(CO)_3(C_5Me_5)$ Radical with Thiones versus Thiols: A Theoretical and Experimental Investigation

Kengkaj Sukcharoenphon,[†] Damian Moran,[‡] Paul v. R. Schleyer,*[,‡] James E. McDonough,[†] Khalil A. Abboud,*[,§] and Carl D. Hoff*[,†]

Departments of Chemistry, University of Miami, Coral Gables, Florida 33124, University of Georgia, Athens, Georgia 30602, and University of Florida, Gainesville, Florida 32611

Received July 8, 2003

2-Pyridinethione (2-mercaptopyridine, H-2mp) undergoes rapid oxidative addition with 2 mol of the 17-electron organometallic radical $^{\bullet}Cr(CO)_3Cp^*$ (where $Cp^* = C_5Me_5$), yielding hydride H–$Cr(CO)_3Cp^*$ and thiolate (η^1-2mp)$Cr(CO)_3Cp^*$. In a slower secondary reaction, (η^1-2mp)$Cr(CO)_3Cp^*$ loses CO generating the N,S-chelate complex (η^2-2mp)$Cr(CO)_2Cp^*$ for which the crystal structure is reported. The rate of 2-pyridine thione oxidative addition with $^{\bullet}Cr(CO)_3Cp^*$ (abbreviated $^{\bullet}$Cr) in toluene best fits rate $= k_{obs}$[H-2mp][$^{\bullet}$Cr]; k_{obs}(288 K) $= 22 \pm 4$ M^{-1} s^{-1}; $\Delta H^{\ddagger} = 4 \pm 1$ kcal/mol; $\Delta S^{\ddagger} = -40 \pm 5$ cal/mol K. The rate of reaction is the same under CO or Ar, and the reaction of deuterated 2-pyridine thione (D-2mp) shows a negligible (inverse) kinetic isotope effect ($k_D/k_H = 1.06 \pm 0.10$). The rate of decarbonylation of (η^1-2mp)$Cr(CO)_3Cp^*$ forming (η^2-2mp)$Cr(CO)_2Cp^*$ obeys simple first-order kinetics with k_{obs} (288 K) $= 3.1 \times 10^{-4}$ s^{-1}, $\Delta H^{\ddagger} = 23 \pm 1$ kcal/mol, and $\Delta S^{\ddagger} = +5.0 \pm 2$ cal/mol K. Reaction of 4-pyridine thione (4-mercaptopyridine, H-4mp) with $^{\bullet}Cr(CO)_3Cp^*$ in THF and CH_2Cl_2 also follows second-order kinetics and is approximately 2–5 times faster than H-2mp in the same solvents. The relatively rapid nature of the thione versus thiol reactions is attributed to differences in the proposed 19-electron intermediate complexes, [$^{\bullet}$(S═C_5H_4N—H)$Cr(CO)_3Cp^*$] versus [$^{\bullet}$(H—S—C_6H_5)$Cr(CO)_3Cp^*$]. In comparison, reactions of pyridyl disulfides occur by a mechanism similar to that followed by aryl disulfides involving direct attack of the sulfur–sulfur bond by the metal radical. Calorimetric data indicate Cr–SR bond strengths for aryl and pyridyl derivatives are similar. The experimental conclusions are supported by B3LYP/6-311+G(3df,2p) calculations, which also provide additional insight into the reaction pathways open to the thione/thiol tautomers. For example, the reaction between H$^{\bullet}$ radical and the 2-pyridine thione S atom yielding a thionyl radical is exothermic by ≈30 kcal/mol. In contrast, the thiuranyl radical formed from the addition of H$^{\bullet}$ to the 2-pyridine thiol S atom is predicted to be unstable, eliminating either H$^{\bullet}$ or HS$^{\bullet}$ without barrier.

Introduction

It is known that low valent 17-electron (17-e$^-$) organometallic radical complexes undergo more rapid ligand substitution reactions than the corresponding saturated 18-electron (18-e$^-$) complexes.[1] The slower 17-e$^-$ oxidative addition reactions, however, are more complex than the simple substitution processes, as in addition to the initial binding event, they also require activation of the coordinating molecule. As a result, a greater range of 17-e$^-$ oxidative addition reaction mechanisms is possible, some of which are illustrated for the $^{\bullet}Cr(CO)_3Cp^*$ (abbreviated as $^{\bullet}$Cr) 17-e$^-$ radical in the Scheme 1 general mechanism.

Reversible formation of an initial 19-e$^-$ (or 18 + δ) adduct,[1] such as that shown in the Scheme 1 central reaction, is presumed to be the first step in all mechanisms. This initially formed complex can undergo homolytic cleavage of the A−B bond, as depicted in the top Scheme 1 reaction channel and as is the case for direct cleavage of the relatively weak PhS−SPh[2] sulfur−sulfur bond. For stronger MeS−SMe,[2] RS−H[3] or H−H[4] bond attack by a single $^{\bullet}$Cr, as

* To whom correspondence should be addressed. E-mail: choff@jaguar.ir.miami.edu (C.D.H.).
† University of Miami.
‡ University of Georgia.
§ University of Florida.

(1) (a) Tyler, D. R. *Acc. Chem. Res.* **1991**, *24*, 325. (b) Geiger, W. E. *Acc. Chem. Res.* **1995**, *28*, 351. (c) Sun, S.; Sweigart, D. A. *Adv. Organomet. Chem.* **1996**, *40*, 171. (d) The authors would like to thank one of the referees for suggesting that some of the proposed intermediate complexes might be more properly viewed as 18 + δ rather than 19-e$^-$ adducts.

10.1021/ic034791s CCC: $25.00
Published on Web 11/18/2003

Scheme 1. Potential •Cr(CO)$_3$Cp* Reaction Channels

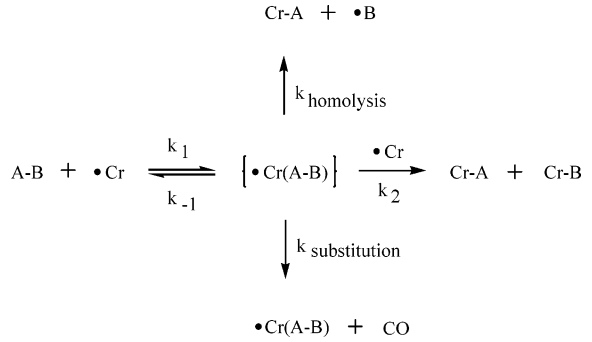

shown in the top Scheme 1 mechanism, would be slow due to the large bond strength differences between A−B and Cr−A.[5] However, attack of 2 mol of radical on the substrate, shown in the middle Scheme 1 pathway, can lead to the ternary {Cr•(A−B)•Cr} transition state and net third-order reaction kinetics.•Cr(CO)$_3$Cp* oxidative addition reactions can also occur with rate-determining ligand substitution, as shown in the lower Scheme 1 pathway. For example, under an argon atmosphere (the reaction channel was suppressed under CO), the relatively small ligand H_2S was proposed to displace CO, forming the substituted •Cr(H_2S)(CO)$_2$Cp* radical.[6] However, except where ligand substitution can occur, or relatively weak substrate bonds are broken, the Cr• radical appears to favor oxidative additions that are second-order in metal radical. It was, therefore, surprising to find at the start of these studies that even under CO atmosphere "2-mercaptopyridine" underwent relatively rapid oxidative addition reactions with Cr• species that were apparently first-order in metal concentration, thus presenting an apparent contradiction to each of the three general mechanisms in Scheme 1.

The compound "2-mercaptopyridine" (H-2mp) displays reactivity consistent with both thiol and thione tautomeric forms:[7]

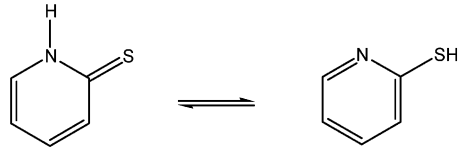

(1)

2-pyridine thione 2-pyridine thiol

The solid-state structure[8] is a doubly hydrogen bonded dimeric thione form:

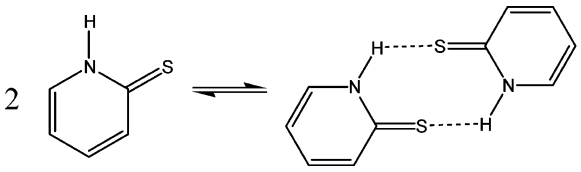

(2)

The thione dimer is also present in concentrated nonpolar solvent solutions, while the thione monomer is favored in polar solvents. The thiol form is often cited as being more stable in nonpolar solvents and the gas phase;[9] however, recent experimental and theoretical data show that, even in dilute nonpolar solutions, it is the monomeric thione, and not the thiol form, that is predominant.[10]

The R_2C═S bond is known to be a versatile receptor[11] of "thiophilic radicals". In particular, trialkyltin radicals are trapped by thiaxanthates[12] and rapidly release radicals as shown in reaction 3:

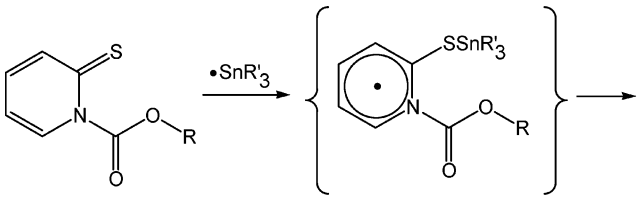

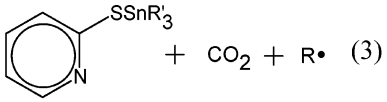

(3)

While a range of transition metal/pyridine thione complexes have been prepared,[13] the authors are not aware of reactions between transition metal based radicals and pyridine thiones. Relavent related work includes Abrahamson and co-workers'[14] report of synthetic chemistry based on the 2,2′-dibenzothiazolyl disulfide plus [CpW(CO)$_3$]$_2$ reaction, yielding CpW(CO)$_3$(η^1-SCSN(C$_6$H$_4$)). Progress in the synthesis and characterization of CpCr(CO)$_2$(η^2-*N*,*S*-SCSN(C$_6$H$_4$)) (obtained from the reaction between solutions of •Cr(CO)$_3$Cp and disulfides) and several related derivatives was reported by Goh and co-workers[15] while this study was in progress.

Theoretical and experimental studies of gas-phase radical additions to heterocyclic rings with C═O and C═S func-

(2) Ju, T. D.; Capps, K. B.; Lang, R. F.; Roper, G. C.; Hoff, C. D. *Inorg. Chem.* **1997**, *36*, 614.
(3) Ju, T. D.; Lang, R. L.; Roper, G. C.; Hoff, C. D. *J. Am. Chem. Soc.* **1996**, *118*, 5328.
(4) Capps, K. B.; Bauer, A.; Kiss, G.; Hoff, C. D. *J. Organomet. Chem.* **1999**, *586*, 23.
(5) Hoff, C. D. *Coord. Chem. Rev.* **2000**, *206*, 451.
(6) Capps, K. B.; Bauer, A.; Ju, T. D.; Hoff, C. D. *Inorg. Chem.* **1999**, *38*, 6130.
(7) The compound H-2mp as purchased from Aldrich Chemical Co. is titled as 2-mercaptopyridine (the alternative name provided is 2-pyridinethiol) and drawn as a thiol tautomer. While the chemical literature abounds with references to the thiol/thione tautomerization reaction, the authors were unaware of the significance of this reaction and only later learned that there is no solution phase experimental evidence for the existence of a thiol tautomer (see ref 10).
(8) (a) Penfold, B. R. *Acta Crystallogr.* **1953**, *6*, 707. (b) Ohms, U.; Guth, H.; Kutoglu, A.; Scheringer, C. *Acta Crystallogr., Sect. B* **1982**, *38*, 831.
(9) Katrizky, A. R.; Jug, K.; Oniciu, D. C. *Chem. Rev.* **2001**, *101*, 1421.
(10) Moran, D.; Sukcharoenphon, K.; Puchta, R.; Schaefer, H. F., III; Schleyer, P. v. R.; Hoff, C. D. *J. Org. Chem.* **2002**, *67*, 9061.
(11) Crich, D.; Quintero, L. *Chem. Rev.* **1989**, *89*, 1413.
(12) Barton, D. H. R.; McCrombie, S. W. *J. Chem. Soc., Perkin Trans. 1* **1975**, 1574.
(13) For a recent example of preparation and structures of transition metal derivatives of "pyridine-2-thiol" see: (a) Umakoshi, K.; Yamasaki, T.; Fukuoka, A.; Kawano, H.; Ichikawa, M.; Onishi, M. *Inorg. Chem.* **2002**, *41*, 4093. (b) Kettler, P. B.; Chang, Y.; Rose, D.; Zubieta, J.; Abrams, M. J. *Inorg. Chim. Acta* **1996**, *244*, 199.
(14) Brandenburg, K. L.; Heeg, M. J.; Abrahamson, H. B. *Inorg. Chem.* **1987**, *26*, 1064.
(15) Goh, L. Y.; Weng, Z.; Leong, W. K.; Vittal, J. J. *J. Am. Chem. Soc.* **2002**, *124*, 8804.

tionalities by the Turecek group[16] have shown that H atom addition to ring carbon atoms appears to be the preferred kinetic and thermodynamic reaction channel. However, different behavior is expected for transition metal complexes due to the fact that most metal complexes form stronger bonds to −OR or −SR than they do to −R.[17] Furthermore, in terms of reaction site preference, organotransition metal radicals would be expected to display "thiophilic" character similar to that of the eq 3 triorganotin radical. This paper reports synthetic, kinetic, and thermodynamic, as well as computational, investigations of •Cr(CO)$_3$Cp* radical reactions with N-heterocyclic thiols and disulfides.

Experimental Section

General. Manipulations were carried out under argon using standard Schlenk tube and glovebox techniques. Toluene, hexadeuterobenzene, THF, and heptane were purified by distillation from sodium benzophenone under argon. Methylene chloride was distilled from P_2O_5 under argon. Infrared data were measured on a Perkin-Elmer series 2000 FTIR spectrometer using either the normal beam or the microscope system described earlier[6] for kinetic studies. Calorimetric measurements were made using a Setaram C-80 Calvet calorimeter or a Guild solution calorimeter. NMR data were obtained on a Bruker AVANCE 300 MHz spectrometer. Mass spectra were obtained on a VG MASSLAB TRIO-2 spectrometer using FAB of solutions. Analytical data were obtained from Galbraith Laboratories, Inc. 2,2′-Pyridine disulfide (2,2′-PySSPy), 4,4′-pyridine disulfide (4,4′-PySSPy), 2-mercaptopyridine (H-2mp), and 4-mercaptopyridine (H-4mp) were purchased from Aldrich Chemical Co. and purified by low-temperature recrystallization in mixtures of methylene chloride/heptane. The complex [Cr(CO)$_3$Cp*]$_2$ was prepared as described in the literature.[18]

Preparation of (η^2-2mp)Cr(CO)$_2$Cp*. In the glovebox, 0.1563 g (0.288 mmol) of solid [Cr(CO)$_3$Cp*]$_2$ and 0.0618 g of 2,2′-PySSPy (0.281 mmol) were weighed into a 25 mL flask. To this was added 15 mL of freshly distilled toluene. Initial infrared data showed bands at 2014, 1956, and 1923 cm^{-1} assigned to (η^1-2mp)Cr(CO)$_3$Cp*. The reaction mixture was stirred for 1−2 h and turned dark red during this time. FTIR spectroscopy showed complete disappearance of bands due to •Cr(CO)$_3$Cp* [1994 and 1893 cm^{-1}] and (η^1-2mp)Cr(CO)$_3$Cp* [2014, 1956, and 1923 cm^{-1}] and buildup of new bands assigned to the dicarbonyl product (η^2-2mp)Cr(CO)$_2$Cp* [1944 and 1874 cm^{-1}]. Evaporation of solvent yielded a crude crop of brown crystals [0.13 g ≈ 65% yield]. Mass spectral data (FAB$^+$): m/e = 297 = M$^+$ assignable to Cp*Cr(η^2-2mp)$^+$ and M$^+$ − Cp* = 162. ^{1}H NMR data (C_6D_6): 7.39 (d, 1H-*Py*); 6.49 (t, 1H-*Py*); 6.27 (d, 1H-*Py*); 5.99 (t, 1H-*Py*); and 1.41 (s, 15H-*Cp**) ppm. Recrystallization by slow cooling of a methylene chloride/heptane solution of the crude product gave an analytically pure sample. Calcd (Found) %: C, 57.78 (57.28); H, 5.42 (5.66); N, 3.96 (3.83).

Attempted Reaction of (η^2-2mp)Cr(CO)$_2$Cp* with CO. A solution of (η^2-2mp)Cr(CO)$_2$Cp* in toluene was prepared in the glovebox and transferred via stainless steel cannula to a high-pressure FTIR cell under argon atmosphere. The initial spectrum showed bands at 1944 and 1874 cm^{-1} due to (η^2-2mp)Cr(CO)$_2$Cp*. The cell was then filled with CO at ≈40 atm pressure and monitored for a 24 h period. No change in the spectrum was observed. In particular, bands assigned to (η^1-2mp)Cr(CO)$_3$Cp* at 2014, 1956, and 1923 cm^{-1} were not found under these conditions.

Crystal Growth for X-ray Structure of (η^2-2mp)Cr(CO)$_2$Cp*. A saturated toluene solution of (η^2-2mp)Cr(CO)$_2$Cp* was prepared in the glovebox, transferred to a 7 mm tube, layered with heptane, and finally capped with a plastic cap. The tube was placed in a large screw-cap test tube fitted with a Teflon gasket and sealed in the glovebox under argon. The test tube containing the 7 mm tube was transferred to a freezer (−20 °C) for a period of a month. During that time, well formed red-brown crystals developed. The crystals were taken into the glovebox, the liquor removed by syringe and the crystals washed with heptane and stored over degassed paraffin oil.

Preparation of (η^1-4mp)Cr(CO)$_3$Cp* and Crystal Growth for X-ray Structure. Preparation of (η^1-4mp)Cr(CO)$_3$Cp* was done in a strictly analogous fashion to that described above for (η^2-2mp)Cr(CO)$_2$Cp*, with the noted difference that the initially formed tricarbonyl (η^1-4mp)Cr(CO)$_3$Cp* (ν_{CO} in toluene = 2013, 1958, 1925 cm^{-1}) was stable. Mass spectral data (FAB$^+$): m/e = 382 = M$^+$ assignable to protonated Cp*Cr (CO)$_3$(η^1-4mp)$^+$; M$^+$ − CO = 354; M$^+$ − 2CO = 326; M$^+$ − 3CO = 297; and M$^+$ − Cp*-2CO = 163. ^{1}H NMR data (C_6D_6): 8.42 (d, 2H-*Py*); 7.44 (d, 2H-*Py*); and 1.43 (s, 15H-*Cp**) ppm. Crystals suitable for structural determination were grown by preparing a saturated solution of the complex at room temperature in heptane and filtering it into a clean Schlenk tube which was then stored for two weeks in the freezer. During that time, well formed yellow-orange crystals precipitated. The crystals were taken into the glovebox, the liquid removed by syringe and the crystals washed with heptane and stored under degassed paraffin oil.

Structural Determination of (η^2-2mp)Cr(CO)$_2$Cp* and (η^1-4mp)Cr(CO)$_3$Cp*. Data were collected at 173 K on a Siemens SMART PLATFORM equipped with a CCD area detector and a graphite monochromator utilizing Mo Kα radiation (λ = 0.71073 Å). Cell parameters were refined using up to 8192 reflections. A hemisphere of data (1381 frames) was collected using the ω-scan method (0.3° frame width). The first 50 frames were remeasured at the end of data collection to monitor instrument and crystal stability (maximum correction on I was <1%). Absorption corrections by integration were applied on the basis of measured indexed crystal faces.

The structure was solved by the Direct Methods in *SHELXTL5*[19] and refined using full-matrix least-squares. The non-H atoms were treated anisotropically, whereas the hydrogen atoms were calculated in ideal positions and were riding on their respective carbon atoms. The S-pyridine ligand is found to be disordered and was refined in two parts (related by a pseudomirror plane). Their site occupation factors were dependently refined to 0.88(1) for the major part, and consequently 0.12(1) for the minor part. The geometry of the minor part of the disorder was constrained to be always equivalent to the major part geometry. All atoms of the minor parts had their isotropic thermal parameter refined as one variable. Minor disorder is also observed on the Cp* and carbonyl ligands but could not be resolved. The centrosymmetric space group *Pnma* was considered for structure solution, but refinement on that proved to be not acceptable because of the poor refinement and the requirement that both the carbonyl and Cp* ligands be disordered as well. A total of 222 parameters (with 18 constraints) were refined in the final cycle of refinement using 3179 reflections with $I > 2\sigma(I)$ to yield R1 and

(16) (a) Wolken, J. K.; Turecek, F. *J. Phys. Chem. A* **2001**, *105*, 8352. (b) Wolken, J. K.; Turecek, F. *J. Am. Chem. Soc.* **1999**, *121*, 6010.
(17) Simoes, J. A. M.; Beauchamp, J. L. *Chem. Rev.* **1990**, *90*, 629.
(18) Watkins, W. C.; Jaeger, T.; Kidd, C. E.; Fortier, S.; Baird, M. C.; Kiss, G.; Roper, G. C.; Hoff, C. D. *J. Am. Chem. Soc.* **1992**, *114*, 907.
(19) Sheldrick, G. M. *SHELXTL5*; Bruker-AXS: Madison, WI, 1998.

wR2 values of 4.74% and 11.97%, respectively. Refinement was done using F^2.

The structure of (η^1-4mp)Cr(CO)$_3$Cp* was determined using similar techniques, and a total of 222 parameters were refined in the final cycle of refinement using 3201 reflections with $I > 2\sigma(I)$ to yield R1 and wR2 of 3.77% and 8.34%, respectively. Refinement was done using F^2. A summary of the crystal structure experimental data for both complexes is provided in the text, and full data are available as Supporting Information.

Kinetic Studies. Reactions were done using the FTIR microscope/reactor system that has been described in detail elsewhere[6] using either batch reactions or continuous flow techniques. Reported data are the averages of typically five independent measurements at each temperature. A representative procedure is outlined below.

Rate of Reaction of •Cr(CO)$_3$Cp* with H-2mp and H-4mp. 2•Cr(CO)$_3$Cp* + H-2mp → (η^1-2mp)Cr(CO)$_3$Cp* + H−Cr(CO)$_3$Cp*. A typical study of the rate of this reaction was performed in toluene solution at 15 °C. Initial concentration based on formal concentrations 3.5 mM in [Cr(CO)$_3$Cp*]$_2$ and 1.75 mM [H-2mp]$_2$ are calculated[10,18] to contain initial concentrations at 15 °C corresponding to 0.67 mM [Cr(CO)$_3$Cp*]$_2$ and 5.66 mM •Cr(CO)$_3$Cp* for the metal complex and 0.83 mM [H-2mp]$_2$ and 1.84 mM H-2mp monomer for the thione. No attempt was made to refine kinetic data on the basis of initial dimeric species in solution because following the first half-life (which was generally more rapid than the sampling rate), these solutions evolved to contain predominantly monomeric species in solution. Monomer/dimer exchange rates are known to be extremely fast for both systems.[1,10] Dissociation of both species is more extensive in CH_2Cl_2 and THF than it is in toluene.

The rate of reaction was followed by sampling every 12 s from the batch reactor where reaction was initiated by injection of the thione to a solution of the chromium radical under a positive pressure of either argon or carbon monoxide. The rate of decay of starting material paralleled the rate of buildup of products, and clear spectroscopic isosbestic points were observed, indicative of no intermediate or secondary products during the initial reaction. No dependence of the rate of reaction on CO versus argon atmosphere was observed. Under these conditions, a rate law first-order in both reagents was found with the following values of $k_{obs} = 21.9 \pm 3.8$ M^{-1} s^{-1} at 15 °C, 18.8 ± 2.7 M^{-1} s^{-1} at 5 °C, and 14.5 ± 2.0 M^{-1} s^{-1} at −5 °C. Reactions studied by continuous flow FTIR from $t = 1$ to $t = 40$ s under-pseudo first-order conditions of excess pyridine thione gave a derived second-order rate constant at 22 °C of 28 M^{-1} s^{-1}. Experiments done at 15 °C under identical conditions using H-2mp or D-2mp showed $k_D/k_H = 1.06 \pm 0.10$.

Solution Calorimetric Studies. A representative procedure is given for measurements of ΔH_{rxn} of •Cr(CO)$_3$Cp* and 2,2′-PySSPy; analogous procedures were used in other reactions. The liquid mixing cell of the Setaram C-80 calorimeter was taken into the glovebox and loaded with 2.2 mL of a 31.3 mM toluene solution of •Cr(CO)$_3$Cp* and 2.0 mL of a 12.4 mM toluene solution of 2,2′-PySSPy. The cell was sealed, taken out of the glovebox, and loaded in the calorimeter. Following thermal equilibration (≈2 h), the reaction was initiated by rotating the calorimeter. An initial rapid exothermic response was followed by a slower endothermic return to baseline. After approximately 90 min, data collection was stopped, and the contents of the reaction were examined by FTIR spectroscopy. FTIR data showed only bands due to (η^2-2mp)Cr(CO)$_2$-Cp* at 1944 and 1874 cm^{-1} and to unreacted excess •Cr(CO)$_3$Cp* at 1994 and 1893 cm^{-1}. The average value of seven runs gave a measured energy of reaction of -21.0 ± 1.2 kcal/mol. This value was adjusted to a final value of $-22.3 + 1.4$ kcal/mol following corrections for pressure, volume, and dilution terms during the calorimetry in the closed Calvet calorimeter.

Computational Details. The goal of our theoretical calculations was to determine relative and absolute energies of the thiopyridyl radicals obtained by H-atom abstraction from either radical, and the energies associated with H-atom addition to 2-pyridine thione and thiol, as well as their gas-phase electron affinities. Density functional theory (DFT), in particular B3LYP, has been shown to provide accurate equilibrium geometries and good harmonic vibrational frequencies for a broad range of molecules, radicals, and ions,[20] and B3LYP/6-311+G(3df,2p) was used to optimize geometries and compute frequencies (all frequencies are unscaled). Minima were characterized as stationary points and zero point vibrational energies (ZPEs) obtained using frequency analysis.[21] GIAO−B3LYP/6-311+G(3df,2p) nucleus independent chemical shifts (NICS)[22] were computed 1 Å above the center of six membered rings to probe their ring currents, i.e., aromaticity. The Gaussian 98 program suite[23] was used throughout.

Results

The Kinetics of Reaction Between •Cr(CO)$_3$Cp* and 2- and 4-Pyridine Thiones. As shown in eq 4, oxidative addition of 1 equiv of 2-pyridine thione to 2 equiv of •Cr yields 1 equiv each of H−Cr and RS−Cr products:

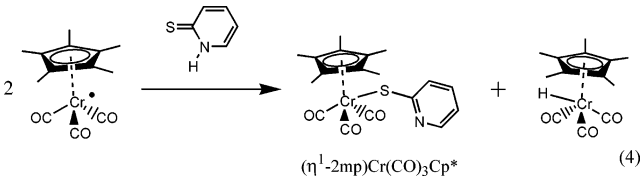

(4)

The tricarbonyl thiolate product initially formed is not stable and undergoes a slow, secondary decarbonylation reaction yielding (η^2-2mp)Cr(CO)$_2$Cp*:

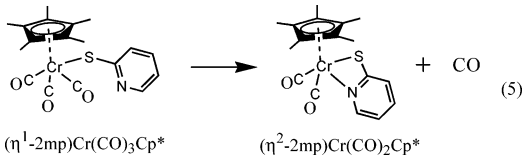

(5)

Reaction 5 is significantly slower than reaction 4, and kinetic data on the two separate processes are readily obtained. Kinetic data for the rate of decarbonylation in reaction 5 are discussed later, as is the crystal structure of the final product from reactions 4 and 5, (η^2-2mp)Cr(CO)$_2$Cp*.

The reaction 4 kinetic studies were typically done under the special case that 2[•Cr] = [thione], with initial [•Cr] ≅ 7 mM. As discussed in the Experimental Section, these solutions consist predominantly of 2-mp monomers during

(20) (a) Koch, W.; Holthausen, M. C. *A Chemist's Guide to Density Functional Theory*; Wiley-VCH: Weinheim, 2000. (b) Schleyer, P. v. R.; Allinger, N. L.; Clark, T.; Gasteiger, J.; Kollman, P. A.; Schaefer, H. F., III; Schreiner, P. R. *The Encyclopedia of Computational Chemistry*; John Wiley & Sons, Ltd.: Chichester, U.K., 1998.
(21) Hehre, W. J.; Radom, L.; Pople, J. A.; Schleyer, P. v. R. *Ab Initio Molecular Orbital Theory*; John Wiley & Sons: New York, 1986.
(22) (a) Schleyer, P. v. R.; Maerker, C.; Dransfeld, A.; Jiao, H.; Hommes, N. J. R. v. E. *J. Am. Chem. Soc.* **1996**, *118*, 6317. (b) Schleyer, P. v. R.; Jiao, H.; Hommes, N. J. R. v. E.; Malkin, V. G.; Malkina, O. L. *J. Am. Chem. Soc.* **1997**, *119*, 12669. (c) Schleyer, P. v. R.; Manoharan, M.; Wang, Z.-X.; Kiran, B.; Jiao, H.; Puchta, R.; Hommes, N. J. R. v. E. *Org. Lett.* **2001**, *3*, 2465.

Table 1. Collected Rate Constants for Reaction of H-2mp and H-4mp with $Cr(CO)_2Cp^*$

thione	solvent	T (°C)	k_{obs} (M^{-1} s^{-1})
H-2mp	toluene	−5	14.5
H-2mp	toluene	5	18.8
H-2mp	toluene	15	21.9
D-2mp	toluene	15	23.2
H-2mp	THF	15	19.3
H-4mp	THF	15	92
H-2mp	CH_2Cl_2	15	7
H-4mp	CH_2Cl_2	15	12
H-2mp	toluene	22	28

the reaction's first half-life but may also contain 2-mp dimers. Following the first half-life (which was generally faster than the sampling rate), the rate of reaction corresponds to that of the monomeric species, with a second-order rate law providing the best fit to experimental data: $d[P]/dt = k_{obs}[^{\bullet}Cr][thione]$. Experimental data from −5 to 22 °C are collected in Table 1. The rate of reaction 4 was found to be the same under argon or CO atmospheres, and the D-2mp reaction had a negligible inverse kinetic isotope effect: $k_D/k_H = 1.06 \pm 0.10$. During the course of the experiment, there was no FTIR evidence of intermediates, and isosbestic points were maintained. On the basis of these observations, any intermediate radical species are certainly present at ≤2%; i.e., their concentration is ≤0.1 mM, and it is likely that they are present at even lower levels than this since attempts[24] to detect them by ESR spectroscopy have so far been unsuccessful.

Toluene was the preferred solvent for H-2mp kinetic studies, but due to H-4mp's virtual insolubility in this solvent, THF and CH_2Cl_2 were used to study the latter. To allow valid comparison, H-2mp was also studied in THF and CH_2Cl_2. However, as shown in Table 1, there was only a small solvent dependence observed for the H-2mp rates of reaction: toluene ≈ THF > CH_2Cl_2.

The activation of H-4mp, as shown in eq 6, was found to be faster than reaction 4 by factors of ≈5 (THF) and 2 (CH_2Cl_2) (Table 1).

$$\text{H-4mp} + 2^{\bullet}Cr(CO)_3Cp^* \rightarrow (\eta^1\text{-4mp})Cr(CO)_3Cp^* + H{-}Cr(CO)_3Cp^* \quad (6)$$

Qualitative competition studies, in which the chromium radical was reacted with equimolar mixtures of H-2mp and H-4mp, confirmed the more rapid rate of reaction of the 4-isomer. A secondary chelate forming reaction, analogous to eq 5, was (of course) not observed for the $(\eta^1\text{-4mp})Cr(CO)_3Cp^*$ complex. The crystal structure of $(\eta^1\text{-4mp})Cr(CO)_3Cp^*$ was determined and is discussed later.

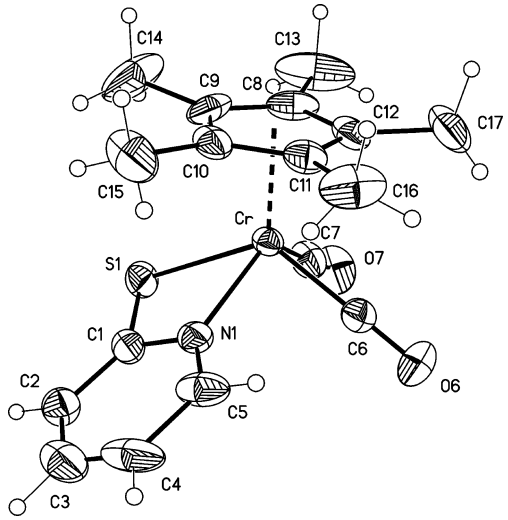

Figure 1. ORTEP drawing of $(\eta^2\text{-2mp})Cr(CO)_2Cp^*$.

Kinetic Studies of Oxidative Addition of 2,2′-Pyridine Disulfide Followed by Decarbonylation of $(\eta^1$-2mp)Cr-$(CO)_3Cp^*$. Oxidative addition of •Cr to the 2,2′-PySSPy sulfur−sulfur bond, as shown in reaction 7, occurs readily at room temperature in toluene solution:

$$2^{\bullet}Cr(CO)_3Cp^* + 2,2'\text{-PySSPy} \rightarrow 2(\eta^1\text{-2mp})Cr(CO)_3Cp^* \quad (7)$$

The initial product of reaction 7, $\{(\eta^1\text{-2mp})Cr(CO)_3Cp^*\}$, shows identical spectroscopic properties to that produced from the thione in reaction 4. In similar fashion, decarbonylation occurs smoothly in a second step producing $(\eta^2\text{-2mp})Cr(CO)_2Cp^*$ as in reaction 5. For reaction 7, the rate law $dP/dt = k_{obs}[^{\bullet}Cr][2,2'\text{-PySSPy}]$ was valid with average second-order rate constant values: 0.0615 M^{-1} s^{-1} at 25.0 °C; 0.027 M^{-1} s^{-1} at 15 °C; and 0.013 M^{-1} s^{-1} at 5.0 °C. These data yield activation parameters $\Delta H^{\ddagger} = +12 \pm 1$ kcal/mol and $\Delta S^{\ddagger} = -24 \pm 2$ cal/mol K. Accurate measurement of the secondary reaction 5 rate is possible by employing high [2,2′-PySSPy] concentrations, which increase the rate of $(\eta^1\text{-2mp})Cr(CO)_3Cp^*$ production via reaction 7. The rate of $(\eta^1\text{-2mp})Cr(CO)_3Cp^*$ decarbonylation, as shown in eq 5, was the same whether it was prepared via reaction 4 or reaction 7. For reaction 5, the rate law $dP/dt = k_{obs}[(\eta^1\text{-2mp})Cr(CO)_3Cp^*]$ was valid, with average values of the first-order rate constant, $k_{obs} = 6.7 \times 10^{-5}$ s^{-1} at 5 °C, 3.13×10^{-4} s^{-1} at 15 °C, and 1.2×10^{-3} s^{-1} at 25 °C, that yielded $\Delta H^{\ddagger} = 23 \pm 1$ kcal/mol and $\Delta S^{\ddagger} = 5 \pm 2$ cal/mol K values. These thermochemical parameters are comparable to the values ($\Delta H^{\ddagger} = 27$ kcal/mol and $\Delta S^{\ddagger} = 3.1$ cal/mol K) obtained for the decarbonylation of $CpW(CO)_3$(S-2Py), where 2Py = 2-mercaptopyridine. We note that for both reactions 5 and 7, experiments performed under a pressure of 1.3 atm CO occurred at an identical rate to those studied under argon atmosphere, implying kinetically irreversible loss of CO.

(23) Frisch, M. J.; Trucks, G. W.; Schlegel, H. B.; Scuseria, G. E.; Robb, M. A.; Cheeseman, J. R.; Zakrzewski, V. G.; Montgomery, J. A., Jr.; Stratmann, R. E.; Burant, J. C.; Dapprich, S.; Millam, J. M.; Daniels, A. D.; Kudin, K. N.; Strain, M. C.; Farkas, O.; Tomasi, J.; Barone, V.; Cossi, M.; Cammi, R.; Mennucci, B.; Pomelli, C.; Adamo, C.; Clifford, S.; Ochterski, J.; Petersson, G. A.; Ayala, P. Y.; Cui, Q.; Morokuma, K.; Malick, D. K.; Rabuck, A. D.; Raghavachari, K.; Foresman, J. B.; Cioslowski, J.; Ortiz, J. V.; Stefanov, B. B.; Liu, G.; Liashenko, A.; Piskorz, P.; Komaromi, I.; Gomperts, R.; Martin, R. L.; Fox, D. J.; Keith, T.; Al-Laham, M. A.; Peng, C. Y.; Nanayakkara, A.; Gonzalez, C.; Challacombe, M.; Gill, P. M. W.; Johnson, B. G.; Chen, W.; Wong, M. W.; Andres, J. L.; Head-Gordon, M.; Replogle, E. S.; Pople, J. A. *Gaussian 98*, revision A.7; Gaussian, Inc.: Pittsburgh, PA, 1998.
(24) Sukcharoenphon, K.; McDonough, J. E.; Walker, L.; Angerhofer, A.; Hoff, C. D. Work in progress.

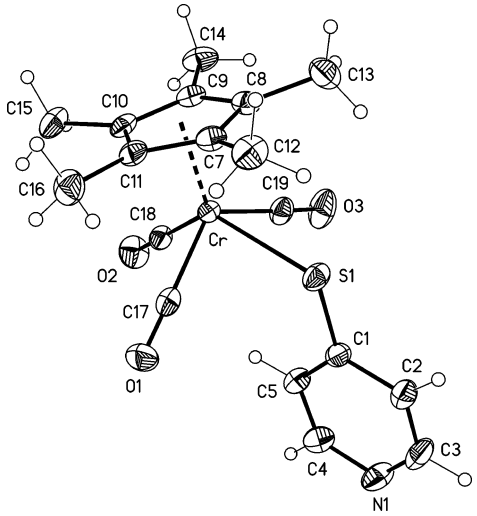

Figure 2. ORTEP drawing of (η^1-4mp)Cr(CO)$_3$Cp*.

Table 2. Crystallographic Data and Structure Refinement for (η^2-2mp)Cr(CO)$_2$Cp* and (η^1-4mp)Cr(CO)$_3$Cp*

	(η^2-2mp)Cr(CO)$_2$Cp*	(η^1-4mp)Cr(CO)$_3$Cp*
chemical formula	$C_{17}H_{19}CrNO_2S$	$C_{18}H_{19}CrNO_3S$
fw	353.39	381.40
cryst syst	orthorhombic	triclinic
space group	*Pna*2$_1$	$P\bar{1}$
a, Å	13.7818(6)	8.5515(4)
b, Å	8.7397(4)	9.2058(4)
c, Å	13.8672(6)	11.5446(5)
α, deg	90	76.791(1)
β, deg	90	82.232(1)
γ, deg	90	89.464(1)
V, Å^3	1670.3(1)	876.45(7)
Z	4	2
ρ_{calcd}, Mg/m^3	1.405	1.445
μ, mm^{-1}	0.815	0.787
crystal size, mm^3	0.13 × 0.15 × 0.26	0.02 × 0.13 × 0.21
color	red-brown	yellow-orange
	Diffractometer	
T, K	173(2)	193(2)
λ, Å	0.71073	0.71073
θ range, deg	2.75−27.50	1.83−27.49
no. reflns	10703	7927
indep reflns	3608	3925
abs correction	integration	integration
	Solution Refinement	
data/restraints/params	3608/18/222	3925/0/222
GOF	1.060	1.023
R1[a]	0.0474	0.0377
wR2[b] [$I > 2\sigma(I)$]	0.1197	0.0834
largest diff peak, e Å^{-3}	0.483	0.325
largest diff hole, e Å^{-3}	−0.356	−0.343

[a] $R1 = \Sigma(||F_o| - |F_c||)/\Sigma|F_o|$. [b] $wR2 = [\Sigma[w(F_o^2 - F_c^2)^2]/\Sigma[w(F_o^2)^2]]^{1/2}$.

Structures of (η^2-2mp)Cr(CO)$_2$Cp* and (η^1-4mp)Cr(CO)$_3$Cp*. The (η^2-2mp)Cr(CO)$_2$Cp* and (η^1-4mp)Cr(CO)$_3$Cp* complexes are shown in Figures 1 and 2, with selected structural parameters summarized in Tables 2−4 (full data are available as Supporting Information). Like many other 7-coordinate Cp* metal carbonyl complexes, both complexes may be described as having a 4:3 piano-stool geometry about the chromium center. Although the (η^2-2mp)Cr(CO)$_2$Cp* Cr−S (2.44 Å) and Cr−CO (1.83 Å [av]) bonds are slightly shorter than in (η^1-4mp)Cr(CO)$_3$Cp* (2.46 and 1.87 [av] Å, respectively), both complexes have structures comparable to those reported for the analogous [CpCr(CO)$_2$(μ-SPh)]$_2$ (2.45 Å [av] and 1.85 Å [av], respectively) and CpCr(CO)$_2$(η^2-*N*,*S*-SCSN(C$_6$H$_4$)) (2.49 and 1.85 [av] Å, respectively) Cr(II) complexes.[25,15] The (η^1-4mp)Cr(CO)$_3$Cp* structure is expected to be similar to that of the intermediate (η^1-2mp)-Cr(CO)$_3$Cp*, which proceeded to form (η^2-2mp)Cr(CO)$_2$-Cp* and could not be isolated. The (η^1-4mp)Cr(CO)$_3$Cp* Cr−S1−C1 angle (112.39°) is wider than that for (η^2-2mp)Cr(CO)$_2$Cp* (79.32°). The (η^2-2mp)Cr(CO)$_2$Cp* chelate complex structure's S1−C1−N1 angle (109.7°) and S1−C1 bond length (1.72 Å) are smaller than those in the parent pyridine disulfide (2-mpd[26]) structure (111.5° and 1.78 Å, respectively). Thus, chelation results not only in steric changes about the metal, but in distortion of the organic fragment as well.

Table 3. Selected Bond Lengths (Å) and Angles (deg) for (η^2-2mp)Cr(CO)$_2$Cp*

Cr−N1	2.062(4)	N1−C1	1.339(7)
Cr−S1	2.4422(14)	N1−C5	1.353(8)
Cr−C6	1.835(4)	C1−C2	1.393(7)
Cr−C7	1.835(5)	C4−C5	1.400(9)
S1−C1	1.720(6)	C2−C3	1.377(11)
O6−C6	1.161(5)	C3−C4	1.371(12)
O7−C7	1.159(6)	Cr−Cp* (centroid)	1.856

Cr−S1−C1	79.32(18)	C1−C2−C3	115.9(6)
Cr−N1−C5	134.9(4)	C2−C3−C4	123.1(5)
Cr−N1−C1	103.8(4)	C3−C4−C5	118.0(7)
S1−Cr−N1	67.13(14)	S1−Cr−C6	124.55(14)
S1−C1−N1	109.7(3)	S1−Cr−C7	79.24(15)
S1−C1−C2	128.1(5)	N1−Cr−C6	83.15(18)
N1−C1−C2	122.1(5)	N1−Cr−C7	120.75(19)
C1−N1−C5	121.3(4)	Cr−C6−O6	179.2(4)
N1−C5−C4	119.4(7)	Cr−C7−O7	177.7(4)
C7−Cr−C6	77.7(2)		

Thermochemistry of Oxidative Addition of Pyridine Disulfides and Pyridine Thiones. Reaction enthalpies were measured by solution calorimetry in toluene, with equilibrium data[10,18] for [H-2mp]$_2$ and [Cr(CO)$_3$Cp*]$_2$ dissociation used to correct for the possible presence of dimeric species.

$$2^{\bullet}Cr(CO)_3Cp^* + 2,2'\text{-PySSPy} \rightarrow 2CO + 2(\eta^2\text{-2mp})Cr(CO)_2Cp^* \quad (8)$$
$$\Delta H = -22.3 \pm 1.4 \text{ kcal/mol}$$

$$2^{\bullet}Cr(CO)_3Cp^* + 4,4'\text{-PySSPy} \rightarrow 2(\eta^1\text{-4mp})Cr(CO)_3Cp^* \quad (9)$$
$$\Delta H = -30.9 \pm 1.6 \text{ kcal/mol}$$

$$2^{\bullet}Cr(CO)_3Cp^* + \text{H-2mp} \rightarrow CO + H{-}Cr(CO)_3Cp^* + (\eta^2\text{-2mp})Cr(CO)_2Cp^* \quad (10)$$
$$\Delta H = -14.2 \pm 0.6 \text{ kcal/mol}$$

Reaction 10 was measured using slow Calvet calorimetric techniques, in which the final reaction product is (η^2-

(25) Goh, L. Y.; Tay, M. S.; Mak, T. C.; Wang, R. J. *Organometallics* **1992**, *11*, 1711.
(26) Raghavan, N. V.; Seff, K. *Acta Crystallogr.* **1977**, *B33*, 386.

Table 4. Selected Bond Lengths (Å) and Angles (deg) for (η^1-4mp)Cr(CO)$_3$Cp*

Cr−S1	2.4623(6)	C1−C2	1.404(3)
S1−C1	1.757(2)	C1−C5	1.387(3)
Cr−C17	1.892(2)	C2−C3	1.380(4)
Cr−C18	1.867(2)	C4−C5	1.386(3)
Cr−C19	1.849(2)	N1−C4	1.334(3)
O1−C17	1.141(3)	N1−C3	1.333(3)
O1−C18	1.148(3)	Cr−Cp* (centroid)	1.842
O1−C19	1.145(3)		

Cr−S1−C1	112.39(8)	C17−Cr−C18	81.95(9)
C5−C1−C2	116.2(2)	C17−Cr−C19	121.63(10)
S1−C1−C2	117.85(18)	C18−Cr−C19	79.54(10)
S1−C1−C5	125.88(17)	Cr−C17−O1	178.9(2)
C4−N1−C3	115.0(2)	Cr−C18−O2	178.7(2)
C1−C5−C4	119.7(2)	Cr−C19−O3	177.9(2)
C1−C2−C3	119.2(2)	S1−Cr−C17	75.42(7)
C2−C3−N1	125.3(2)	S1−Cr−C18	127.62(7)
C5−C4−N1	124.7(2)	S1−Cr−C19	73.7(7)

2mp)Cr(CO)$_2$Cp*. Measurement of the same reaction using rapid isoperibol calorimetry yielded the enthalpy of the first step of reaction 10, as shown in eq 11:

$$2^{\bullet}\text{Cr(CO)}_3\text{Cp*} + \text{H-2mp} \rightarrow \text{H−Cr(CO)}_3\text{Cp*} + (\eta^1\text{-2mp})\text{Cr(CO)}_3\text{Cp*} \quad (11)$$

$$\Delta H = -17.5 \pm 1.5 \text{ kcal/mol}$$

Subtraction of eq 10 from eq 11 leads to straightforward calculation of the decarbonylation enthalpy, albeit with relatively high error:

$$(\eta^2\text{-2mp})\text{Cr(CO)}_2\text{Cp*} + \text{CO} \rightarrow (\eta^1\text{-2mp})\text{Cr(CO)}_3\text{Cp*} \quad (12)$$

$$\Delta H = -3.3 \pm 2.1 \text{ kcal/mol}$$

Addition of twice reaction 12 to reaction 8 yields reaction 13:

$$2^{\bullet}\text{Cr(CO)}_3\text{Cp*} + \text{2,2′-PySSPy} \rightarrow 2(\eta^1\text{-2mp})\text{Cr(CO)}_3\text{Cp*} \quad (13)$$

$$\Delta H = -28.9 \pm 6.3 \text{ kcal/mol}$$

Since the calculated enthalpy of reaction 13 is derived from several combined reactions, it incorporates a relatively high experimental error. Nevertheless, it is not significantly different from the enthalpy of reaction 9. Oxidative addition of H-2mp, as shown in eq 11, can be compared to the earlier reported[3] value for oxidative addition of thiophenol:

$$2^{\bullet}\text{Cr(CO)}_3\text{Cp*} + \text{H−SPh} \rightarrow \text{H−Cr(CO)}_3\text{Cp*} + \text{PhS−Cr(CO)}_3\text{Cp*} \quad (14)$$

$$\Delta H = -18.6 \pm 1.8 \text{ kcal/mol}$$

Oxidative addition of pyridine disulfides, as shown in eqs 9 and 13, can be compared to that reported[2] earlier for phenyl disulfide:

$$2^{\bullet}\text{Cr(CO)}_3\text{Cp*} + \text{PhS−SPh} \rightarrow 2\text{PhS−Cr(CO)}_3\text{Cp*} \quad (15)$$

$$\Delta H = -26.6 \pm 3.0 \text{ kcal/mol}$$

The relatively close values for these enthalpies of reaction indicate no significant difference in bond strength when the Cr−S−arene bond (35 ± 3.0 kcal/mol)[2] is replaced by Cr−S-pyridine.

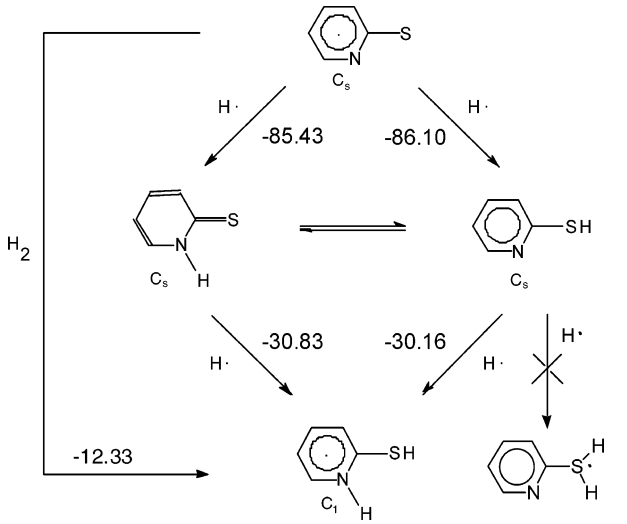

Figure 3. Thione and thiol B3LYP/6-311+G(3df,2p) + ZPE radical reaction enthalpies. Geometries computed at the same level.

Computed Radical Reactivities and Radical Anion Stabilities. In the gas phase, 2-pyridinethiol is 2.6 kcal/mol (CCSD[T]/cc-pVTZ//B3LYP/6-311+G(3df,2p) + ZPE) more stable than 2-pyridinethione, with the competing influences of aromaticity (present in 2-pyridinethiol) and bond enthalpy (N−H vs S−H) leading to a relatively small thiol/thione tautomeric preference.[10] The enthalpy of gas phase H-atom addition to, or abstraction from, either the thiol or thione, shown in Figure 3, simply reflects this tautomeric preference (0.66 kcal/mol at B3LYP/6-311+G(3df,2p) + ZPE), since in either case the same radical product forms. Note that, in Figure 3, hydrogen atom addition to ring carbons is not considered as the transition metal radicals we are modeling are thiophilic and (unlike H) the M−S bond is stronger than the M-CR$_3$ bond.[17] With the expectation of locating a T-shaped thiuranyl radical, we computed a structure with a H-atom added to the 2-pyridinethiol sulfur. However, at B3LYP/6-311+G(3df,2p) such a radical is not stable with respect to either H or SH radical elimination. Related studies have shown that R$_3$S type radicals are not stable unless the radical center is surrounded by electron withdrawing groups. In contrast, H-atom addition to 2-pyridinethione yields a radical with only two groups on sulfur, and the reaction enthalpy is ∼30 kcal/mol favorable.

The B3LYP/6-311+G(3df,2p) electron affinity of the thione derivative is predicted to be 15.78 kcal/mol + ZPE greater than the thiol tautomer. 2-Pyridinethione and 2-pyridinethiol radical anion NICS values, shown in Figure 4, are large and positive indicating that both molecules are antiaromatic. For reference, the NICS value 1 Å above the ring centers of 2-pyridinethiol, 2-pyridinethione, benzene, pyridine, and phenol are −8.8, −3.5, −10.1, −10.1, and −9.6 ppm. Addition of an electron to 2-pyridinethiol, which is aromatic, "switches" the ring current paratropic. As both thiol and thione become antiaromatic following electron binding,

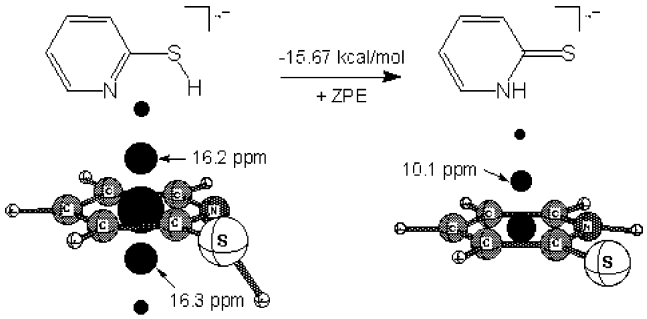

Figure 4. 2-Pyridinethione/thiol radical anion B3LYP/6-311+G(3df,2p) + ZPE relative stability and nucleus independent chemical shifts (NICS). Geometries and frequencies computed at the same level. The large, positive NICS show that both species are antiaromatic.

the loss of thiol aromaticity is responsible for the greater electron affinity of the thione tautomer, which originally is not aromatic.

Discussion

This work was begun to investigate the role of N donor proximity on the kinetics and thermodynamics of organometallic radical •Cr(CO)$_3$Cp* oxidative addition with pyridine disulfides and "thiols", as compared with their nonheterocyclic counterparts. Early on, a much greater "2-mercaptopyridine" reaction rate was observed as compared with thiophenol, butanethiol,[3] and even hydrogen sulfide.[6] It seemed possible that this might be ascribed to the known ability of amines and pyridines to accelerate some reactions of thiols.[27] However, no such acceleration was observed when •Cr(CO)$_3$Cp* was reacted with PhSH in the presence of 10 equiv of pyridine.[28] While not a strong argument against participation of the "2-mercaptopyridine" nitrogen atom, where the local concentration and orientation of the N atom could play a crucial role, the observation that "4-mercaptopyridine" reacted even faster than the 2-isomer provided more convincing evidence that three-center H-bonding was not responsible for the increased heterocyclic thiol/thiones reactivity.

Several months into the work, the inorganic investigators "discovered" that 2-mercaptopyridine underwent thiol/thione tautomerization[9] reactions, as shown in eq 1. Experimental and theoretical[10] investigations showed that while the thiol form is favored in the gas phase, the thione form is present in nonpolar solvents. The thione tautomer shown in eq 1, therefore, has two conceivable sites for initial •Cr(CO)$_3$Cp* attack, the N—H or C═S bonds. However, attack at the N—H bond would be expected to follow kinetics similar to other third-order reactions of the chromium radical,[5] and Bordwell[29] has shown that in DMSO the thione N—H bond is stronger than the thiophenol S—H bond. Furthermore, an insignificant inverse kinetic isotope effect ($k_D/k_H = 1.06 \pm 0.10$) was observed in the rate of D-2mp oxidative addition. Therefore, a strong role of N—H or N—D atom transfer in the reaction transition state seemed unlikely.

Scheme 2. Proposed Mechanism of H-4mp Oxidative Addition with 2 mol of •Cr(CO)$_3$Cp* Generating H—Cr(CO)$_3$Cp* and (η^1-4Mp)Cr(CO)$_3$Cp* as Final Products

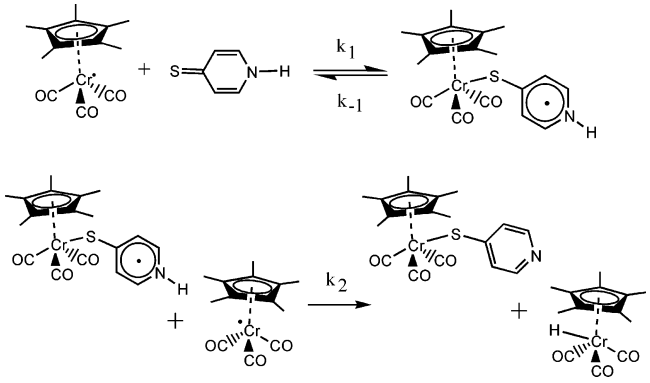

Attempts to explain the observed first-order dependence on metal radical concentration by a ligand substitution pathway such as that shown in the lower Scheme 1 reaction channel could be discounted for two reasons: (i) the rate of reaction was the same under CO or Ar, and (ii) the rate of reaction was faster than H_2S or PMe_2Ph ligand substitution reactions.[6] The central Scheme 1 pathway can in principle display either first- or second-order dependence on metal radical concentration. The rate expression derived for oxidative addition by the central mechanism in Scheme 1 is shown in eq 16:

$$d[P]/dt = \frac{k_1 k_2 [\bullet Cr]^2 [A-B]}{k_{-1} + k_2 [\bullet Cr]} \qquad (16)$$

In all studies to date, the limiting third-order rate law $d[P]/dt = [k_1k_2/k_{-1}][\bullet Cr]^2[A-B]$ has been followed implying $k_{-1} \gg k_2[\bullet Cr]$. The intermediate adduct dissociates back to starting materials more rapidly than it is attacked by a second mole of radical, and the transition state occurs in the second step. However, if that situation should be reversed and $k_2[\bullet Cr] \gg k_{-1}$, then eq 16 would reduce to $d[P]/dt = k_1[\bullet Cr][A-B]$. Under those conditions, the rate-determining step would occur at initial adduct formation. That can occur if either the initial adduct is particularly stable (k_{-1} is smaller than expected), or if attack on the adduct is faster (k_2 larger than expected).

The most plausible mechanism consistent with our data (experimental and computational) and literature studies is shown in Scheme 2.

The first step involves rapid formation of an initial adduct between the chromium radical and H-4mp, presumed to be similar to the (η^1-4mp)Cr(CO)$_3$Cp* structure shown in Figure 2, but with the difference that an H atom is still located on the N atom of the heterocycle and that an unpaired electron (originally on •Cr) is present and delocalized into the thione ring system. The 2—5-fold faster net reaction of H-4mp (see Table 1) than H-2mp was surprising and would appear to rule out direct neighboring group participation by some types

(27) Patai, S. *The Chemistry of the Thiol Group*; Wiley: New York, 1974.
(28) Sukcharoenphon, K.; McDonough, J. E.; Hoff, C. D. Unpublished results.
(29) Bordwell, F. G.; Singer, D. L.; Satish, A. V. *J. Am. Chem. Soc.* **1993**, *115*, 3543.

of hydrogen bonding as an important factor in the reaction. The proposed intermediate radical adduct {•Cr−thioneN−H} could be viewed as {Cr−thiolateN−H•}, in which a H• is weakly bound to the thiopyridine complex N atom. The bound H• should have a reduced N−H bond strength (≈30 kcal/mol, as discussed below) and be readily transferred to a second mole of •Cr in the k_2 step. Steric factors would be expected to favor attack of a second mole of •Cr for H-4mp versus H-2mp in the k_2 step and may be responsible for its slightly accelerated rate.

Theoretical calculations provide additional insight into the type of mechanism shown in Scheme 2 as shown in Figure 3. Calculated gas-phase stabilities favor the thiol tautomer by ≈0.66 kcal/mol (B3LYP/6-311+G(3df,2p) + ZPE), but as discussed elsewhere[10] solvation energies favor the thione in solution. The enthalpy of •H addition to •2mp is ≈86 kcal/mol for both tautomers, which is clearly too high to allow direct attack by •Cr. We note that this predicted value compares well with Bordwell's[29] N−H BDE solution phase (DMSO) estimate of 81 kcal/mol.

Computational data summarized in Figure 3 are also used to estimate the enthalpy of •H addition to the following: (i) S═C of the thione ($\Delta H° = -30.83$ kcal/mol), (ii) N atom of the thiol ($\Delta H° = -30.16$ kcal/mol), and (iii) H−S of the thiol ($\Delta H° \geq 0$ kcal/mol). The reduction of the H-2mp 85.43 kcal/mol N−H BDE to 30.83 kcal/mol in •2mpH$_2$ implies that there is no thermodynamic barrier to attack of •Cr in the k_2 step, and this can also be used to make a rough estimate of the •Cr addition to thione enthalpy. It would be expected to be less exothermic than the −30 kcal/mol value calculated, since the H−S−arene (79 kcal/mol) bond[32] is stronger than the Cr−SPh (35 kcal/mol) bond. Assuming $BDE_{\{X-S-C_5H_4N\}}/BDE_{\{Y-S-C_5H_4N\}} = BDE_{\{^{\bullet}X-S-C_5H_4N\}}/BDE_{\{^{\bullet}Y-S-C_5H_4N\}}$ leads to the estimation that the enthalpy of •Cr addition to the thione would be ≈−13 kcal/mol. This would imply an added stability for the proposed 19-electron thione adduct, since earlier estimates of formation of adducts between ·Cr and L were on the order of ≈−5 kcal/mol.[5]

H-atom addition to the 2-pyridinethiol sulfur did not lead to a stable adduct, as the resultant thiuranyl radical is not stable with respect to either ·H or ·SH elimination. Since it is expected that ·Cr would attack at S in preference to N, this is in keeping with the increased reactivity of the thione versus the thiol tautomers. Data in Figure 3 also allow calculation of the enthalpy of addition of H_2 to the ·2mp radical to yield the ·2mpH$_2$ radical enthalpy = −12.33 kcal/mol. Surprisingly, that is comparable to values for reversible binding of H_2 at transition metal complexes[30] such as $Rh(PR_3)_3Cl$ and $W(PCy_3)_2(CO)_3$ and implies that under appropriate conditions the ·2mp radical should be thermodynamically capable of binding and splitting H_2.

The mechanism shown in Scheme 2 involves direct ·H transfer in the k_2 step; however, an alternative mechanism involving essentially e^-/H^+ transfer could be involved as shown in eqs 17 and 18:

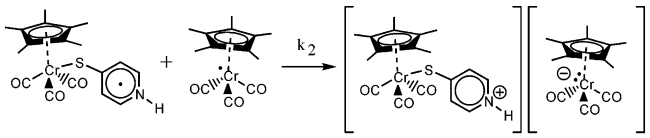

(17)

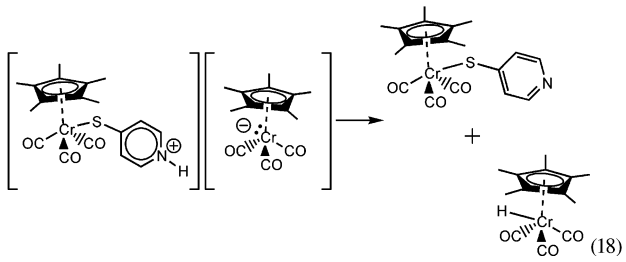

(18)

Reaction 17 involves electron transfer from the initially formed adduct to ·Cr to form an cation/anion pair which would undergo rapid proton transfer in reaction 18 to yield products. Kinetically, ·H atom versus coupled e^-/H^+ transfer can be difficult to distinguish. The lack of significant solvent effect in going from toluene to THF is more in keeping with ·H transfer than an ionic mechanism.

Computational studies also indicate a significant electron affinity for the thione tautomer. Whereas for the neutral molecules the thiol was favored in the gas phase by 0.66 kcal/mol, the anion radical of the thione is favored by 15.67 kcal/mol over the thiol, as shown in Figure 4. Initial binding of ·Cr to the thione fragment may involve partial electron transfer from the metal into the delocalized aromatic ring system. This would be in the direction of forming a zwitterionic $\{Cp^*(CO)_3Cr^+\}\{S-C5H4NH^{\bullet}\}^-$ in the k_1 step. The increased electron affinity calculated for the thione tautomer would indicate increased stability for an adduct of this type relative to the thiol form.

It is of interest to note that the second-order rate constant for oxidative addition of the pyridine thiones studied here is faster than the rate of ligand substitution by reactions such as that shown in eq 19 for L = PMe_2Ph or H_2S:

$$\cdot Cr(CO)_3Cp^* + L \leftrightarrow L\cdot Cr(CO)_3Cp^* \leftrightarrow \cdot Cr(L)(CO)_2Cp^* + CO \quad (19)$$

The reaction 19 second-order rate constants[6] were $k_{obs} \approx 1$ M^{-1} s^{-1}, which is at least an order of magnitude slower than the data in Table 1. Thus, even though both are believed to involve an initial association between the 17-electron radical and substrate, substitution involves full incorporation of ligand binding to the metal with concomitant loss of CO and occurs, at least for bulky ligands, at an apparently slower rate than does the oxidative addition of these thiones. The enthalpy of activation is also higher in the ligand substitution reactions (≈10 kcal/mol for PMe_2Ph and H_2S) than it is for oxidative addition of H-2mp (≈4 kcal/mol).

One of the initial goals of this work was to assess the role of (η^2-2mp)Cr(CO)$_2$Cp* ring strain in its unexpectedly low

(30) Kubas, G. J. *Molecular Hydrogen Complexes*; Kulawehr Publishing: 2002.
(31) Hoff, C. D. *Prog. Inorg. Chem.* **1992**, *40*, 503.
(32) Mukerjee, S. L.; Nolan, S. P.; Hoff, C. D.; de la Vega, R. L. *Inorg. Chem.* **1988**, *27*, 81.

carbonylation enthalpy ($\Delta H = -3.3 \pm 2.1$ kcal/mol). The crystal structure shows signs of strain (acute angles and bond lengthening discussed earlier), and increased thermochemical ring strain was expected for the four-membered metallacyclic ring system, as the N−Cr−S angle ≈ 67 °. For example, we have shown earlier that in the binding of phosphine ligands, strain energies of 8−10 kcal/mol can be found in four-membered rings.[32] Furthermore, for such low valent metal systems, the M−CO bond is stronger than the M−Py bond, even in an unstrained environment.[31] The low enthalpy of carbonylation derived here, therefore, indicates that the apparent ring strain in this chelate is compensated for by stabilizing influences, such as delocalized bonding.

The rate and mechanism of 2,2′-pyridine disulfide oxidative addition ($\Delta H^{\ddagger} = 12 \pm 1$ kcal/mol; $\Delta S^{\ddagger} = -24 \pm 2$ cal/mol K) was similar to that reported earlier for phenyl disulfide ($\Delta H^{\ddagger} = 10$ kcal/mol; $\Delta S^{\ddagger} = -24$ cal/mol K).[2] The slightly slower reaction rate and higher $\Delta H^{\ddagger}$ value observed for pyridine disulfide may be due to blocking of the chromium radicals' approach to the substrates' sulfur−sulfur bond by the heterocyclic N atoms' lone pairs. Thus, attack on the S−S bond of pyridine disulfide is somewhat slower than attack on phenyl disulfide, while oxidative addition to pyridine thione is much faster than to thiophenol.

Conclusion

The Cr−S−arene bond strength does not appear to be significantly influenced when N-heterocycles (2- and 4-pyridine) replace benzene or toluene as the arene. The rate and mechanism of 2,2′-pyridine disulfide oxidative addition is similar to or somewhat slower than that for the analogous phenyl disulfide. The greater 2-mp reaction rates are kinetic in origin, since both experiment and theory confirm that its thiol form is thermodynamically less stable in solution.[10] Computations predict that the greater rate of 2-pyridine thione reaction, as compared with thiols or related substrates, is most likely due to an increased stability of the initially formed adduct between the radical and thione. Additional kinetic, thermodynamic, and theoretical studies aimed at further detailing this process are in progress.

Acknowledgment. Support of this work by the Petroleum Research Fund, administered by the American Chemical Society, the University of Georgia, the U.S. Department of Energy, and the U.S. National Science Foundation (Grant CHE-0209857) is gratefully acknowledged. C.D.H. would like to thank A. Angerhofer and L. Walker at the University of Florida for their assistance with EPR experiments.

Supporting Information Available: Additional figures and tables. This material is available free of charge via the Internet at http://pubs.acs.org.

IC034791S